Optica Applicata, Vol. XLIX, No. 2, 2019
DOI: 10.5277/oa190216

Stable distribution in application to fixational eye movement description

MARTA SZMIGIEL[1*], ALEKSANDRA GRZESIEK[2], AGNIESZKA WYŁOMAŃSKA[2], HENRYK KASPRZAK[1]

[1]Department of Optics and Photonics, Faculty of Fundamental Problems of Technology, Wrocław University of Science and Technology, 50-370 Wrocław, Poland

[2]Faculty of Pure and Applied Mathematics, Hugo Steinhaus Center, Wrocław University of Science and Technology, 50-370 Wrocław, Poland

[*]Corresponding author: marta.szmigiel@pwr.edu.pl

To give an appropriate description of fixational eye movements is a very challenging problem. Over the years authors tried to describe the movements through different methods. The time series of the movements exhibit very characteristic behavior, which is the visible impulses. This may suggest the heavy-tailed distribution behind the data. In this paper on stochastic description of fixational eye movements, the α-stable distribution as the most important member of heavy-tailed family of distributions is proposed. The fixational eye movements together with head movement of both eyes of eight healthy subjects were measured and recorded by use of own designed optical system. Further analysis of changes in position of the pupil center in two-dimensional plane was performed. It was shown that head movement has very small impact on values of stability parameter α of fixational eye movements. The α-stable based analysis can be useful in better understanding of the character of the eye globe dynamics.

Keywords: eye movement, microsaccades, fixational eye movements, α-stable distribution, stochastic modelling.

1. Introduction

Eye globe undergoes continuous fast movements. Contrary to well-known eye movements related to variation in the gaze direction, fixational eye movements concern small involuntary rotations of the eye globe during gaze fixation, when the observed stable point is imaged on the eye fovea. Fixational eye movements are divided into three main types: microsaccades, drift and microtremor [1]. Kinetics and spectral properties of these three types are different and still discussed in the literature [1–3]. Due to a very small amplitude of these movements, their precise measurement and examination is still a challenging task. Some authors demonstrate that drift and tremor are somehow correlated between two eyes [4].

Different methods were introduced and applied for recording and investigating these movements. Most often they used simple eye contact invasive methods [5], non-contact speckle interferometric methods [6], optical sensing methods [7] and event related potentials (ERP) [8, 9].

Authors try to describe movements of the eye with the use of different models. ENGBERT *et al.* [10] introduced an integrated mathematical model for the generation of slow fixational eye movements and microsaccades which was based on the concept of self-avoiding random walks. In the paper of BETTENBUEHL *et al.* [11] it was shown that microsaccades can be formally represented with the use of a continuous wavelet transform. The eye movements are also modeled based on heavy-tailed distributions [12]. Simulations of the saccadic motions have been also solved using the dynamic mesh technique [13].

The α-stable distribution which belongs to the heavy-tailed family is introduced to describe the fixational eye movements in this paper. The class of heavy-tailed distributions is very rich. However, the most important distribution with heavy-tailed property is the α-stable one, also called the stable distribution [14]. Stable laws are important for the fundamental property: the probability density functions of stable laws decay in an asymptotic power-law form. Thus, they appear naturally in the descriptions of many fluctuation processes with largely scattering statistics characterized by bursts or large outliers [15]. The α-stable distribution is very important for modeling data with impulsive behavior. In the fixational eye movements time series this behavior has also been observed, which suggests that this distribution can be successfully considered in their description. It is reasonable to use the distribution for description of microsaccades, where in the time series large observations are clearly visible.

Since MANDELBROT [16] introduced the α-stable distribution in modeling of financial asset returns, numerous empirical studies have been done in different applications. Recently, there is a growing attention from the biology and microbiology to the process called Lévy walk, which is an example of a continuous-time random walk with jumps and waiting times being α-stable distributed and strongly coupled [17, 18]. Furthermore, there are many other interesting applications of α-stable distribution and processes based on it such as applications in plasma fluctuations in fusion devices [19], physics [20] or electrical engineering [21]. The α-stable distributions have also found applications in technical diagnostics [22, 23].

In this paper we demonstrate that the α-stable distribution is appropriate for the considered time series of fixational eye movements. However, in a noninvasive method proposed in the paper, where eye pupil movement was recorded and analyzed, the unavoidable head movements have some influence on obtained results. Therefore, we present that the α-stable-based approach can be useful to describe distribution of fixational eye movements with and without movements of a fastened head.

2. Materials and methods

2.1. Participants

Eight subjects with normal vision participated in this study. For all of the subjects, both eyes were measured. The groups of patients range in age from 25 to 40 years (mean =

31.6 ± 5.3 years, 7 female). Subjects were fully informed about the purpose of the study, all the procedures and their requirements. Informed patients consent was obtained before any measurements were taken. The project was approved by the Ethics Committee of the Wroclaw Medical University (KB 246/2017) and adhered to the Tenets of the Declaration of Helsinki.

2.2. Experiment description

A measurement system was constructed to record fast sequences of images of the iris eye area. High magnification of this images increases the precision of the eye pupil parameters determination, including its center. Based on the change in the position of the pupil center, the movements of the eye were determined.

During the examination, the patient rests his chin and forehead on a specially constructed rigid baseline, which is to minimize movement associated with the movement of head. The head was also fastened by the stressed band pressing the head to the baseline. In addition, the patient was equipped with special adapted glasses that carry information about the movement of the head during the examination. These glasses are situated on the tissues coating orbital surface. Glasses were stabilized in places where bones that form the anterior rim of orbital aperture were most prominent. Structures that were found to define and enhance stabilization were: orbital rim of frontal bone, frontal process of zygomatic bone, nasal bone and orbital rim of maxilla near infraorbital foramen. The use of such glasses, along with the attempt to stabilize the head most possible, gives the ability to isolate the movement of the eyeball from the head movement. Movement of the pupil is compensated by the movement of the reference point set on the glasses.

Video sequences of the pupil were recorded with the use of the fast CCD camera (AOS S-PRI, AOS Technologies AG, Baden Daettwil, Switzerland), which is the main element of the pupil recording system [24]. The system equipped with photolens and infrared retroillumination lightning ensured an optimal pupil image size and visibility of pupillary margin.

The patient was asked to gaze with the examined eye at the motionless fixation point and abstain from blinking for up to 14 seconds, while the recording was made with the speed of 200 frames per second. Due to this eye fixation, the assumption about constant impact of the corneal refraction on the pupil image was made. For each measured eye, 10 video sequences were taken under consideration. During the examination, the unexamined eye reminded covered with no stimulus to fixation, but it could easily stay open.

2.3. Procedure

Each single frame from the video sequence was numerically analyzed with the use of MatLab® software (Mathworks, Natick, MA, USA). Exemplary frame is presented in Fig. 1. Selection of border points of the eye pupil was carried out automatically, with the use of the threshold level procedure. Due to differences in magnification of the pupil,

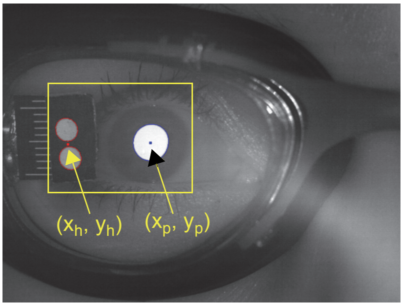

Fig. 1. The exemplary image of the eye pupil with object from the glasses, with marked pupil borders and its center of mass (x_p, y_p) with its close surrounding, along with the objects of the glasses with its center of mass (x_h, y_h) and its close surrounding (±3 pixels in the vertical and horizontal directions). Note that in the experiment, the sequences were recorded with higher magnification to increase precision (size of the recorded picture marked with a rectangle).

calibration of the pupil size was performed for each sequence. The shape of the pupil was treated as a filled plane figure. The center of the pupil (x_p, y_p) was determined using the center of mass equations [25]. Similarly for the object (two circles) of the glasses, the center of mass was determined (x_h, y_h). The difference between those two corresponding coordinates gave the information about position of the pupil center after head movement compensation (x_c, y_c). Calculations of all the mass centers based on one-pixel accuracy of the region of interests profiles give subpixel accuracy of x and y coordinates (components).

Next, all components x_p, y_p, x_c and y_c were subjected to further analysis separately. The presented methodology was applied to the increments of the underlying time series. The appropriate increments of eye position, indicating the fixational eye movements, for data with and without head movement compensation are denoted as Δx_p, Δy_p, Δx_c and Δy_c, respectively.

2.4. Methodology

As it will be shown, the analysed data sets exhibit behavior adequate to so-called heavy-tailed distributions. In the probability theory, heavy-tailed distributions are probability distributions whose tails are not exponentially bounded, which means they have heavier tails than the exponential distribution. In this paper, a member of heavy -tailed family, namely α-stable distribution, was considered. The α-stable distribution is especially useful in description of the data with large observations. We observe this behavior in the analysed time series.

2.4.1. The α-stable distribution

Stable (or α-stable) distributions [14, 26, 27] belong to a four-parameters class of continuous probability distributions. There are few equivalent definitions of α-stable random variables. This paper concentrates on one of them and defines the α-stable distributed random variable through its characteristic function. The random variable X has an α-stable distribution, if the characteristic function of X has the following form [14]:

$$\varphi_X(u) = \begin{cases} \exp\left\{-\sigma^\alpha |u|^\alpha \left[1 - i\beta \operatorname{sign}(u) \tan\frac{\pi\alpha}{2}\right] + i\mu u\right\}, & \alpha \neq 1 \\ \exp\left\{-\sigma |u| \left[1 + i\beta \operatorname{sign}(u) \frac{2}{\pi} \ln|u|\right] + i\mu u\right\}, & \alpha = 1 \end{cases} \tag{1}$$

where $\alpha \in (0, 2]$ is called the stability index, $\sigma > 0$ is the scale parameter, $\beta \in [-1, 1]$ is skewness parameter and $\mu \in R$ is the location.

We remind, in the probability theory, that the characteristics of any real-valued random variable completely defines its probability distribution. If a random variable admits a probability density function (continuous distributed random variable), then the characteristic function is the Fourier transform of the probability density function (PDF), *i.e.*:

$$\varphi_X(u) = \int_{-\infty}^{\infty} \exp(iux) f(x) \mathrm{d}x \tag{2}$$

where $f(x)$ is the probability density function of given random variable.

It is worth to mention that for $\alpha = 2$ the α-stable distribution is the classic Gaussian one. The most known procedure for α-stable distribution parameters estimation utilizes the characteristic function Eq. (1). By comparing the empirical and theoretical characteristic functions, it is possible to estimate the appropriate parameters. This technique is called the regression method and it is one of the effective algorithms to estimate the parameters of α-stable distributions [28].

2.4.2. Testing of the α-stable distribution

In order to prove that the given data can be described by the α-stable distribution we decided to apply the goodness-of-fit statistical tests for the α-stable distribution. Here the Kolmogorov–Smirnov (KS) test based on KS statistic is used which is defined as follows:

$$\mathrm{KS} = \sup_x |F_n(x) - F(x)| \tag{3}$$

where $F(\cdot)$ is the theoretical cumulative distribution function of α-stable distribution and $F_n(\cdot)$ is the empirical cumulative distribution function of the considered sample.

The other test used is based on the statistics which belongs to the Cramer–von Mises family. In general, the statistics from Cramer–von Mises (CvM) family has the following form:

$$\mathrm{CvM} = n\int_{-\infty}^{\infty} \left|F_n(x) - F(x)\right|^2 \psi(x)\,\mathrm{d}F(x) \tag{4}$$

where $\psi(\cdot)$ is a suitable function. For $\psi(x) = |F(x)(1 - F(x))|^{-1}$ the CvM statistics is called Anderson–Darling (AD) statistics [29]. In presented case for both KS and AD tests p_{value} was calculated. For the small p_{vaule} the zero hypothesis was rejected which in the presented case is the assumption of α-stable distribution. In this study, the p_{vaule} of KS and AD goodness-of-fit statistical tests were analysed in order to confirm that the α-stable distribution is acceptable for examined time series of Δx and Δy.

3. Results

The exemplary trajectories obtained by the experiment from the selected sequence are presented in Fig. 2, where Fig. 2**a** demonstrates recorded movements of the pupil center during eye fixation (x_p, y_p), Fig. 2**b** presents recorded movements of the head (x_h, y_h) and Fig. 2**c** demonstrates calculated movements of the pupil center with head move-

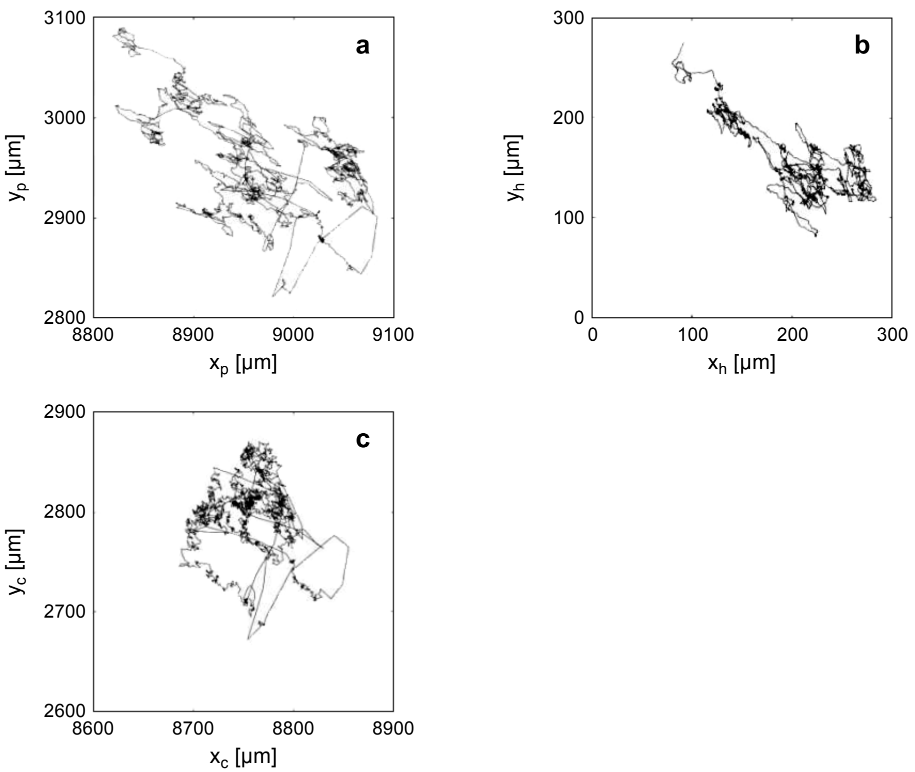

Fig. 2. The exemplary trajectory of recorded movements of the pupil center during eye fixation (x_p, y_p) (**a**), recorded movements of the head (x_h, y_h) (**b**), and calculated movements of the pupil center with head movement compensation (x_c, y_c) (**c**) for selected sequence.

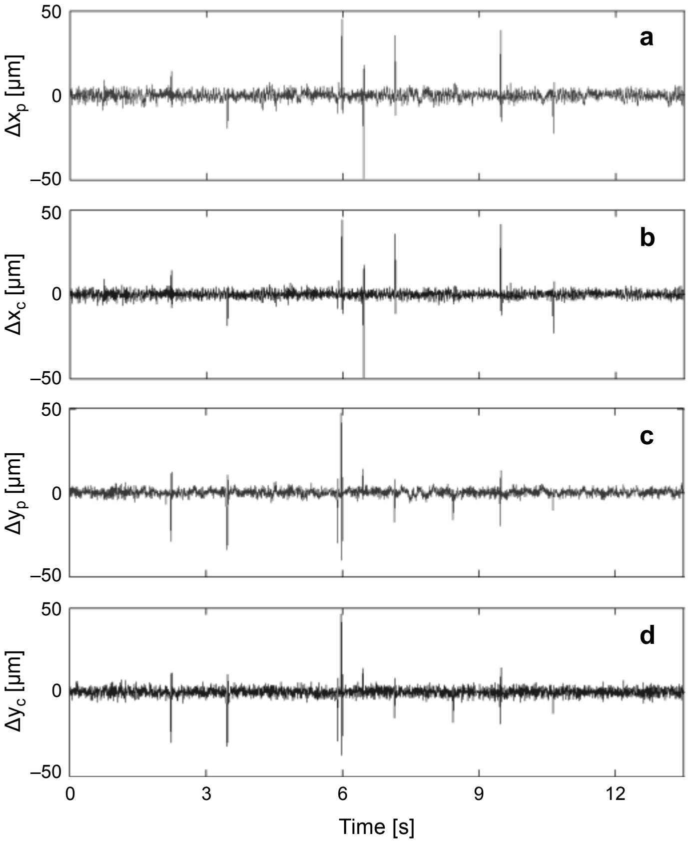

Fig. 3. Time series related to Δx_p (**a**), Δx_c (**b**), Δy_p (**c**) and Δy_c (**d**) component.

ment compensation (x_c, y_c). It is noticeable that positions of a fastened head changes the trajectory of the eye pupil, hence the trajectory on Fig. 2**a** and 2**c** differs in shape. It can also be seen that the range of movements both vertically and horizontally decreased.

Figure 3 shows Δx and Δy components in time, calculated for the same sequence. Again, Fig. 3**a** and 3**c** correspond to data without head movement compensation (Δx_p and Δy_p), while Fig. 3**b** and 3**d** correspond to data with head movement compensation (Δx_c and Δy_c).

For both approaches, the time series presented in Fig. 3 are supposed to have heavy -tailed behavior, the large impulses indicate non-Gaussian behavior. The time plots of other examined time series are similar to those presented in Fig. 2.

To more easily exhibit the distribution of these variables, Fig. 4 presents PDF for Δx_p, Δx_c, Δy_p and Δy_c. For each of the distributions the parameters of the Gaussian distribution and the α-stable distribution were calculated, and the curves of this adjustment are shown in Fig. 4 in the form of a black line (for Gaussian distribution) and gray line

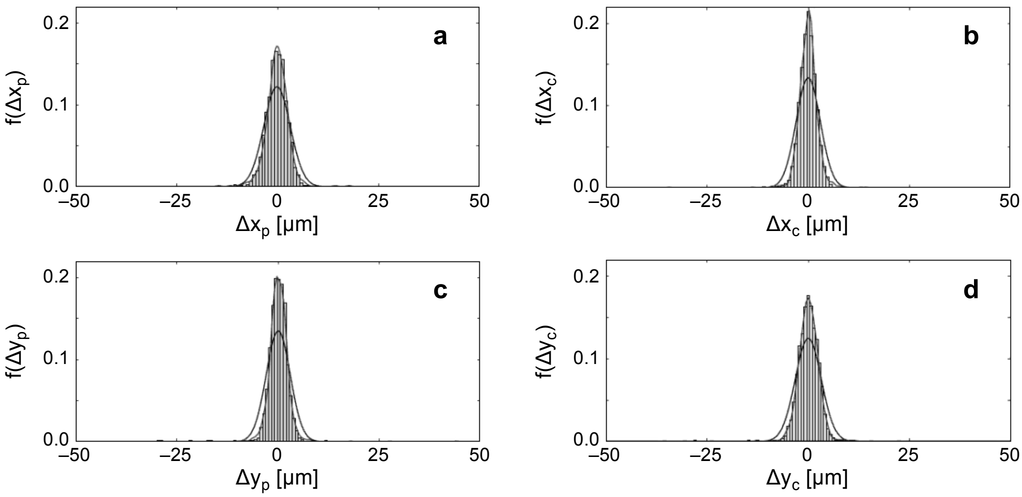

Fig. 4. Probability density for Δx_p (**a**), Δx_c (**b**), Δy_p (**c**) and Δy_c (**d**) component with PDF for Gaussian distribution (black line) and for the α-stable distribution (gray line).

(for the α-stable distribution). It can be seen that the α-stable distribution seems to describe the actual data much better than the Gaussian distribution.

In order to confirm that the α-stable distribution is appropriate for the most of the considered time series, both with and without head movement compensation, the summarizing of the results of KS and AD goodness-of-fit tests applied to Δx and Δy components are presented in Table 1 and Table 2, respectively. More precisely, it is shown for how many sequences it is satisfied that the p-values corresponding to KS test or AD test are greater than the confidence level 5%, which means that the hypothesis of α-stable distribution cannot be rejected.

As one can observe, the Δx component for almost all of the time series exhibits behavior related to α-stable distribution because either both of the tests (KS and AD) or one of the tests (only KS or only AD) do not reject the hypothesis. This appears for

Table 1. Number of sequences (fraction) for which statistical tests do not reject the hypothesis of stable distribution of Δx.

		Number of sequences (fraction)	
	Tests	Left eye	Right eye
Δx_p	KS and AD	57 (71.25%)	54 (67.40%)
	Only KS	0 (0%)	1 (1.25%)
	Only AD	23 (28.75%)	25 (31.25%)
	None of two tests	0 (0%)	0 (0%)
Δx_c	KS and AD	55 (68.75%)	50 (62.50%)
	Only KS	0 (0%)	3 (3.75%)
	Only AD	25 (31.25%)	26 (32.50%)
	None of two tests	0 (0%)	1 (1.25%)

T a b l e 2. Number of sequences (fraction) for which statistical tests do not reject the hypothesis of stable distribution of Δy.

		Number of sequences (fraction)	
	Tests	Left eye	Right eye
Δy_p	KS and AD	63 (78.75%)	73 (91.25%)
	Only KS	0 (0.00%)	0 (0.00%)
	Only AD	16 (20.00%)	6 (7.50%)
	None of two tests	1 (1.25%)	1 (1.25%)
Δy_c	KS and AD	57 (71.25%)	59 (73.75%)
	Only KS	1 (1.25%)	0 (0%)
	Only AD	20 (25.00%)	18 (22.50%)
	None of two tests	2 (2.50%)	3 (3.75%)

the sequences related to both left and right eyes in both approaches, with and without head movement compensation. Similarly is for Δy component.

Figure 5 presents the boxplots of the estimated α parameter from α-stable distribution for each of the considered patients (for left eye). The α parameter is estimated

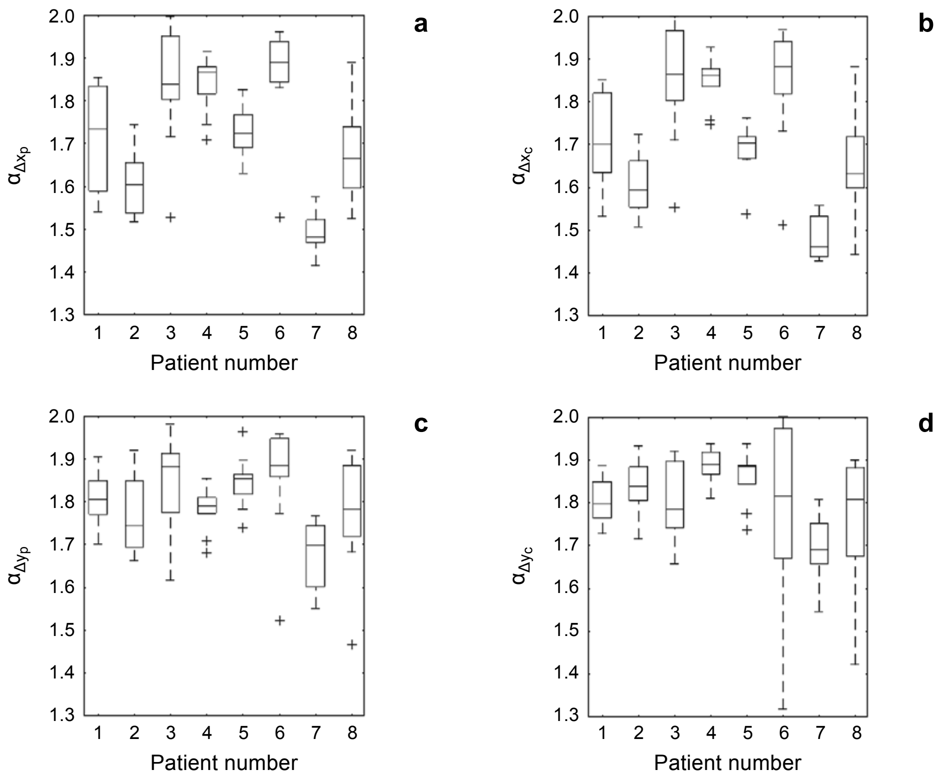

Fig. 5. Boxplots of stable parameter α calculated for Δx_p (**a**), Δx_c (**b**), Δy_p (**c**) and Δy_c (**d**) component from the α-stable distribution for all left eye sequences.

for each sequence separately for Δx and Δy components. Finally, for each patient, the boxplot is taken from 10 considered sequences. As one can see, there are no crucial differences between estimated α parameters for time series related to the case with and without head movement compensation. In order to show the differences between the series corresponding to the cases with and without head movement compensation, we have calculated the simple factor. Namely, for each patient we take the median of the estimated α parameter and calculate the square difference between medians obtained for the series related to the case with and without head movement compensation. Finally, we calculate the mean of obtained square differences for all patients. The factor is calculated separately for Δx and Δy component.

As a result, we obtain the following value of the factor: 0.00049 and 0.00435 for components Δx and Δy, respectively. The small values of the factors for Δx and Δy components indicate the differences between series related to the cases with and without head movement compensation are not substantial.

4. Discussion

Usually fixational eye movements are treated as small, fast rotations of the eye globe, caused by the eye muscles, which produce respective fast transversal movements of the point image over cones in the fovea. However, such approach is very simple and assumes that the eye rotates as a rigid body. In fact, the problem is much more complex. The eye globe and optical structures inside the eye undergo fast deformations.

Irregular corneal deformations due to blood pulsation in the eye structures [30] or microfluctuations in the crystalline lens position during small accommodative movements [31], can produce fast fine transversal movements of image of observed point on the fovea even without activity of the eye muscles. Measured high order aberrations of the eye during fixation [32] shows that transversal movement of the point image on the fovea is very likely the result of complex superposition of the small eye rotations and the fast fluctuations of deformations of the eye optics structures. Microsaccades are clearly the fast eye rotations and produce fast linear transversal movements of point image over the fovea. In the case of tremor, the situation is much more complex and dependence between very fast, small eye rotations and respective transversal displacements of the point image on the fovea is clear.

From this point of view, it is important to realize what is actually measured. Local measurement of small displacements of the eye surface is likely not directly related with the small eye rotations. In this case, the position of the mass center of the pupil image was measured. The position was calculated with the subpixel accuracy as such data describe more objectively eye movements in comparison to their local measurements. Influence of fixational eye movements on visual performance is still intensively examined and discussed by researchers. It would be interesting to deeper investigate the correlation between some visual parameters of the eye and stochastic properties of its fixational movement.

It should be remembered that the movements of the head, which were registered despite a solid support of the forehead and the beard, were natural movements, independent of the will of the examined person. In this examinations we have additionally compensated the data with the synchronously recorded head movements. It is shown that the proposed stochastic analysis of fixational eye movements can describe properly the distribution of analyzed data. Using advanced statistical tests, it has been proved the α-stable distribution can be considered as an appropriate one for description of fixational eye movements both without and with head movements' compensation. Almost all of the examined data exhibited behavior adequate to this distribution. Although values of α parameters differ between specific eyes, they differ insignificantly for measurements with and without head movement compensation.

5. Conclusions

Fixational eye movement can be characterized by using one of the member of a heavy -tailed distribution family, namely α-stable distribution. It was proved, using a variety of statistical methods, that α-stable distribution is the general one appropriate for most of all considered patients. Presented study can be a starting point for more advanced analysis in the context of fixational eye movement description by using statistical methods. Such analysis could be useful in better understanding of the character of the eye globe dynamics and its quantitative characteristics as well as in a new diagnosis tool in oculomotor dysfunction.

Acknowledgements – M. Szmigiel acknowledges that part of her work was supported by the National Science Centre conferred on the basis of the decision number DEC-2013/11/N/ST7/00366 "Anomalous diffusion processes and their applications in real data modelling". A. Wyłomańska and A. Grzesiek would like to acknowledge the support of the National Science Centre OPUS Grant No. UMO-2016/21/B/ST1/00929. The authors are grateful for the clinical protocol of Joanna Przeździecka -Dołyk, O.D., M.D., PhD., FEBO, from Wroclaw Medical University, Poland.

References

[1] Martinez-Conde S., Macknik S.L., Hubel D.H., *The role of fixational eye movements in visual perception*, Nature Reviews Neuroscience **5**, 2004, pp. 229–240, DOI: 10.1038/nrn1348.

[2] Ezenman M., Hallett P.E., Frecker R.C., *Power spectra for ocular drift and tremor*, Vision Research **25**(11), 1985, pp. 1635–1640, DOI: 10.1016/0042-6989(85)90134-8.

[3] Rucci M., Iovin R., Poletti M., Santini F., *Miniature eye movements enhance fine spatial detail*, Nature **447**, 2007, pp. 852–855, DOI: 10.1038/nature05866.

[4] Spauschus A., Marsden J., Halliday D.M., Rosenberg J.R., Brown P., *The origin of ocular microtremor in man*, Experimental Brain Research **126**(4), 1999, pp. 556–562, DOI: 10.1007/s002210050764.

[5] Sheahan N.F., Coakley D., Hegarty F., Bolger C., Malone J., *Ocular microtremor measurement system: design and performance*, Medical and Biological Engineering and Computing **31**(3), 1993, pp. 205–212, DOI: 10.1007/BF02458038.

[6] Ryle J., Al-Kalbani M.A., Collins N., Gopinathan U., Boyle G., Coakley D., Sheridan J., *Compact portable ocular microtremor sensor: design, development and calibration*, Journal of Biomedical Optics **14**(1), 2009, aticle ID 014021, DOI: 10.1117/1.3083435.

[7] Ryle J., Vohnsen B., Sheridan J., *Simultaneous drift, microsaccades, and ocular microtremor measurement from a single noncontact far-field optical sensor*, Journal of Biomedical Optics **20**(2), 2015, article ID 027004, DOI: 10.1117/1.JBO.20.2.027004.

[8] Moshel S., Zivotofsky A.Z., Jin-Rong L., Engbert R., Kurths J., Kliegl R., Havlin S., *Persistence and phase synchronisation properties of fixational eye movements*, The European Physical Journal Special Topics **161**, 2008, pp. 207–223, DOI: 10.1140/epjst/e2008-00762-3.

[9] Sereno S.C., Rayner K., *Measuring word recognition in reading: eye movements and event-related potentials*, Trends in Cognitive Sciences **7**(11), 2003, pp. 489–493, DOI: 10.1016/j.tics.2003.09.010.

[10] Engbert R., Mergenthaler K., Sinn P., Pikovsky A., *An integrated model of fixational eye movements and microsaccades*, Proceedings of the National Academy of Sciences of the United States of America, PNAS **108**(39), 2011, pp. E765–E770, DOI: 10.1073/pnas.1102730108.

[11] Bettenbuehl M., Paladini C., Mergenthaler K., Kliegl R., Engbert R., Holschneider M., *Microsaccade characterization using the continuous wavelet transform and principal component analysis*, Journal of Eye Movement Research **3**(5), 2010, pp. 1–14, DOI: 10.16910/jemr.3.5.1.

[12] Lenz R., *Eye movements and information geometry*, Journal of the Optical Society of America A **33**(8), 2016, pp. 1598–1603, DOI: 10.1364/JOSAA.33.001598.

[13] Boushehrian H.H., Abouali O., Jafarpur K., Ghaffarieh A., Ahmadi G., *Relationship between saccadic eye movements and formation of the Krukenberg's spindle—a CFD study*, Mathematical Medicine and Biology **34**(3), 2017, pp. 293–312, DOI: 10.1093/imammb/dqw007.

[14] Samorodnitsky G., Taqqu M.S., *Stable Non-Gaussian Random Processes*, Chapman & Hall, New York 1994.

[15] Wylomanska A., Chechkin A., Gajda J., Sokolov I.M., *Codifference as a practical tool to measure interdependence*, Physica A **421**, 2015, pp. 412–429, DOI: 10.1016/j.physa.2014.11.049.

[16] Mandelbrot B., *Stable Paretian random functions and the multiplicative variation of income*, Econometrica **29**(4), 1961, pp. 517–543.

[17] Shlesinger M.F., Klafter J., Wong Y.M., *Random walks with infinite spatial and temporal moments*, Journal of Statistical Physics **27**(3), 1982, pp. 499–512, DOI: 10.1007/BF01011089.

[18] Zaburdaev V., Denisov S., Klafter J., *Lévy walks*, Reviews of Modern Physics **87**(2), 2015, p. 483, DOI: 10.1103/RevModPhys.87.483.

[19] Burnecki K., Wylomanska A., Chechkin A., *Discriminating between light- and heavy-tailed distributions with limit theorem*, PLoS ONE **10**(12), 2015, article ID e0145604, DOI: 10.1371/journal.pone.0145604.

[20] Janicki A., Weron A., *Can one see α-stable variables and processes?*, Statistical Science **9**(1), 1994, pp. 109–126.

[21] Stuck B.W., Kleiner B., *A statistical analysis of telephone noise*, The Bell System Technical Journal **53**(7), 1974, pp. 1263–1320, DOI: 10.1002/j.1538-7305.1974.tb02791.x.

[22] Gang Yu, Changning Li, Jianfeng Zhang, *A new statistical modeling and detection method for rolling element bearing faults based on alpha-stable distribution*, Mechanical Systems and Signal Processing **41**(1–2), 2013, pp. 155–175, DOI: 10.1016/j.ymssp.2013.08.015.

[23] Zak G., Wylomanska A., Zimroz R., *Application of alpha-stable distribution approach for local damage detection in rotating machines*, Journal of Vibroengineering **17**(6), 2015, pp. 2987–3002.

[24] Szmigiel M.A., Kasprzak H., *Distribution of parameters of elliptic approximation of the human pupil*, Optica Applicata **45**(1), 2015, pp. 41–50, DOI: 10.5277/oa150104.

[25] Szmigiel M.A., *Measurement of the fixational eye movements based on observation of the eye pupil kinetics*, Interdisciplinary Journal of Engineering Sciences **2**(1), 2014, pp. 5–7.

[26] Nolan J.P., *Fitting data and assessing goodness-of-fit with stable distributions*, Applications of Heavy Tailed Distributions in Economics, Engineering and Statistics, Washington DC 1999.

[27] Weron R., *On the Chambers–Mallows–Stuck method for simulating skewed stable random variables*, Statistics and Probability Letters **28**(2), 1996, pp. 165–171, DOI: 10.1016/0167-7152(95)00113-1.

[28] Koutrouvelis I.A., *Regression-type estimation of the parameters of stable laws*, Journal of the American Statistical Association **75**(372), 1980, pp. 918–928.

[29] Cizek P., Härdle W., Weron R., *Statistical Tools for Finance and Insurance*, 2nd Ed., Springer, Berlin, Heidelberg 2011, DOI: 10.1007/978-3-642-18062-0.

[30] Kowalska M.A., Kasprzak H.T., Iskander D.R., Danielewska M., Mas D., *Ultrasonic* in vivo *measurement of ocular surface expansion*, IEEE Transactions on Biomedical Engineering **58**(3), 2011, pp. 674–680, DOI: 10.1109/TBME.2010.2100819.

[31] Charman W.N., Heron G., *Fluctuations in accommodation: a review*, Ophthalmic and Physiological Optics **8**(2), 1988, pp. 153–164, DOI: 10.1111/j.1475-1313.1988.tb01031.x.

[32] Iskander D.R., Collins M.J., Morelande M.R., Zhu M., *Analyzing the dynamic wavefront aberrations in the human eye*, IEEE Transactions on Biomedical Engineering **51**(11), 2004, pp. 1969–1980, DOI: 10.1109/TBME.2004.834254.

Received January 15, 2019